



NATIONAL RESEARCH CENTRE
«KURCHATOV INSTITUTE»
Institute for High Energy Physics
of the National Research Centre
«Kurchatov Institute»

Preprint 2023-6

V.A. Dorofeev, D.R. Ereemeev, V.G. Gotman, A.V. Ivashin, I.A. Kachaev,
Yu.A. Khokhlov, M.S. Kholodenko, V.F. Konstantinov, V.I. Lisin,
V.D. Matveev, E.V. Nazarov, V.I. Nikolaenko, A.N. Plekhanov,
D.I. Ryabchikov, A.A. Shumakov, V.P. Sugonyaev, A.M. Zaitsev

**An observation of the $f_0(1710)$ meson in the $\omega\phi$ system in the
Pion-Be Interaction at Momentum of 29 GeV**

Submitted to *European Physical Journal A*

Protvino 2023

Abstract

Dorofeev V.A. et al. An observation of the $f_0(1710)$ meson in the $\omega\phi$ system in the Pion-Be Interaction at Momentum of 29 GeV: NRC «Kurchatov Institute» – IHEP Preprint 2023-6. – Protvino, 2023. – p. 18, figs. 13.

The charge-exchange reaction $\pi^-p \rightarrow n\omega(783)\phi(1020)$, $\omega \rightarrow \pi^+\pi^-\pi^0$, $\phi \rightarrow K^+K^-$ is studied with the upgraded VES facility (U-70, Protvino) in the interaction of a 29 GeV pion beam with a beryllium target. The distribution over the invariant mass of the system $M_{\omega\phi}$ shows a near-threshold signal. A partial wave analysis reveals that the scalar state ($J^{PC} = 0^{++}$) dominates in this mass region.

The observed signal can be described with a contribution of the known resonance $f_0(1710)$. Using OPE approximation for the reaction $\pi^-p \rightarrow n f_0(1710)$ the product of branching fractions is found to be: $Br(f_0(1710) \rightarrow \pi\pi) \cdot Br(f_0(1710) \rightarrow \omega\phi) = (4.8 \pm 1.2) \cdot 10^{-3}$.

Аннотация

В.А. Дорофеев и др. Наблюдение $f_0(1710)$ мезона в системе $\omega\phi$ в пион-Be взаимодействии при импульсе 29 ГэВ.: Препринт НИЦ «Курчатовский институт» – ИФВЭ 2023-6. – Протвино, 2023. – 18 с., 13 рис.

На модернизированной установке ВЕС (У-70, Протвино) изучена зарядово-обменная реакция $\pi^-p \rightarrow n\omega(783)\phi(1020)$, $\omega \rightarrow \pi^+\pi^-\pi^0$, $\phi \rightarrow K^+K^-$ во взаимодействии пионного пучка с импульсом 29 ГэВ с бериллиевой мишенью. Распределение по инвариантной массе системы $M_{\omega\phi}$ показывает около-пороговый сигнал. Парциально-волновой анализ выявляет доминирование в этой области масс скалярного состояния $J^{PC} = 0^{++}$. Наблюденный сигнал может быть описан вкладом известного резонанса $f_0(1710)$. Используя приближение ОПО для реакции $\pi^-p \rightarrow n f_0(1710)$, найдено произведение относительных вероятностей: $Br(f_0(1710) \rightarrow \pi\pi) \cdot Br(f_0(1710) \rightarrow \omega\phi) = (4.8 \pm 1.2) \cdot 10^{-3}$

1. Introduction

The sector of scalar mesons occupies a special place in meson spectroscopy. There is uncertainty and redundancy in an SU(3) nonet of scalars, especially for its isosinglet members in the mass region below 2 GeV, with the $f_0(500)$, $f_0(980)$, $f_0(1370)$, $f_0(1500)$, $f_0(1710)$ ([1]) as candidates. Their classification is disputable.

An observation of a near-threshold peak with preferably $J^P = 0^+$ assignment in the $\phi\omega$ invariant mass spectrum in the reaction $e^+e^- \rightarrow J/\psi \rightarrow \gamma\omega\phi$ was reported in the [2] and confirmed in the [3].

A similar signal was reported in [4] in the interaction of pion beam.

with a beryllium target in the VES experiment. Those results are superceeded with this analysis using new data taken with upgraded VES setup.

2. VES setup

The VES is a wide aperture magnetic spectrometer with electromagnetic calorimetry and particles identification (Figure 1) for fixed-target experiments. It is located at a secondary beam line of the U-70 proton synchrotron (Protvino). The data used for the present analysis were taken with a nominal beam momentum 29 GeV and typical spread $\pm 1\%$. The intensity of the beam of negatively charged particles delivered to the experiment during data taking is typically $(1 \dots 2) \cdot 10^6/s$, of which about 98% are π^- , 1.6% K^- , 0.2% \bar{p} and the rest are muons and electrons.

The beam section consists of beam-defining scintillators, Cherenkov threshold counters for the pion/kaon/antiproton identification and few proportional chambers. The PCs serve majorly for the beam particle tracking. Also they are used with the last dipole magnet of the beam line for the P_{beam} measurement. The accuracy of 1% at 30 GeV gives a limited control over nucleon excitation in the target fragmentation kinematic region using the missing mass technique.

A *Be* target has diameter of 45 mm which fits to the beam spot and thickness of 40 mm which is about 10% of both radiation and nuclear interaction lengths. The target is inserted into a hole in an aluminum holder. The holder is a square prism with sizes of $12 \times 12 \times 20 \text{ cm}^3$. The inlet part of the hole is a cylinder, while the outlet is cone. The holder in its turn is placed into a veto box. An inner layer of the box is assembled of *Sci*-counters and an outer is of *Pb/Sci* "sandwich" counters.

The veto is aimed to reject events with the target fragmentation products leaving the target at large angles. The *Sci*-counters are used in a trigger, while the "sandwiches" signals are digitized for the further analysis. The holder suppresses veto firing on recoil protons and delta-electrons.

The veto box with the target is installed in front of the main spectrometer magnet. The forward opening of the target holder and the box matches the aperture of the spectrometer. The dipole magnet has an aperture with a width of about 2 m and height of 1 m, with the integral of vertical field component of about 1.5 T·m at the current of 4 kA.

Two scintillation disks of 70 mm in diameter, so called "Beam Killer" BK1(2), are placed at the inclined beam trajectory downstream the magnet to suppress events without the beam interaction.

A tracking part of the spectrometer includes proportional and drift chambers. They are: three two-coordinate multiwire proportional chambers (MWPC) with an active area of about $40 \times 25 \text{ cm}^2$ and five two-coordinate MWPCs of $60 \times 40 \text{ cm}^2$ at the entrance of the magnet; two small-gap two-planes drift chambers inside the magnet; three stations of drift tubes with diameter of 30 mm, each with two 3-layers planes (coordinates), with dimensions of about $1.5 \times 2 \text{ m}^2$. The momentum resolution of the spectrometer is about 0.5% at 3 GeV and 1.2% at 25 GeV.

The charged secondaries identification is performed with the use of 28-channel Cherenkov counter (Ch-28), with the threshold momentum for the pion of about 3.5 GeV, see [5] for details.

The amount of a material which a γ quantum traverses before reaching the electromagnetic calorimeter (EMC) [6] at the end of the setup is less than 15% of the radiation length. The EMC energy resolution is about 4% and the coordinate resolution in the central part is 3.2 mm at 5 GeV.

Some other systems of the upgraded setup are described in [7],[8].

3. Events selection

The events of the reaction

$$\pi^- Be \rightarrow A \omega \phi \tag{1}$$

with $\omega \rightarrow \pi^+ \pi^- \pi^0$ and $\phi \rightarrow K^+ K^-$ are selected. Here *A* is a neutron plus a nucleus or excited state.

As the recoil neutron is not detected, the event candidates to the exclusive mesons system are required to have four tracks of particles with corresponding charges and two or three γ clusters in the EMC with the energy $E_\gamma > 200 \text{ MeV}$. The energy of the presumably noisy "free" γ_{free} , if present, should not exceed 500 MeV.

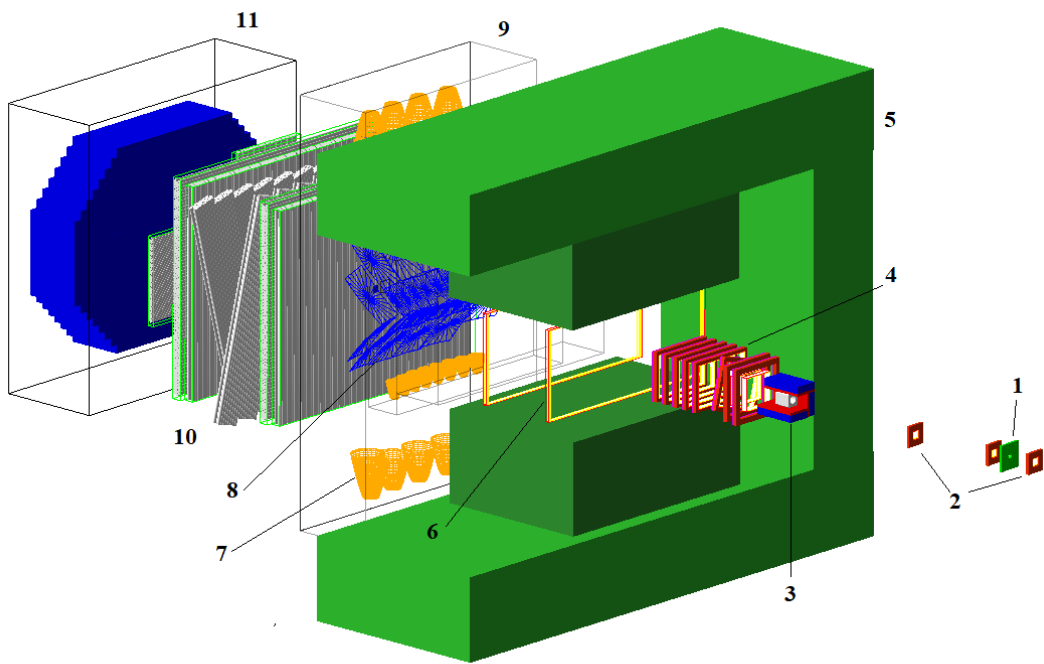


Figure 1. VES setup. Marked are: downstream counter of the beam telescope (1); beam proportional chambers (2); veto box with the target (3); proportional chambers of the spectrometer (4); spectrometer magnet (5); drift chambers (6); light collecting cones (7), mirrors (8) and the body (9) of the Cherenkov counter; drift tubes stations (10); electromagnetic calorimeter (11).

A Gaussian signal of the $\pi^0 \rightarrow \gamma\gamma$ with small background in the invariant mass spectrum has dispersion $\sigma \approx 6.0$ MeV and central position close to the π^0 mass within 0.2 MeV. We take the γ pair with $|M_{\gamma\gamma} - M_{\pi^0}| < 20$ MeV as the π^0 .

To select the events of the beam interaction with the *Be* the reconstructed vertex is required to be in the region of the target. The coordinate resolution for the vertex is typically about 10 mm along the beam direction (close to the *Z*-axis of the setup) and about 1 mm in the perpendicular plane.

As the absolute value of the momentum transferred squared t from the beam to the target is small (see below), the accounting of recoil or target fragments can be omitted to a good approximation in the momentum balance of a reaction. Then the vicinity of the total momentum of detected particles P_{tot} to the P_{beam} is an evidence for a (quasi) exclusive reaction. So the "exclusivity cut" selecting the prominent peak in the P_{tot} distribution (see also below) is imposed: $27.5 < P_{tot} < 31$ GeV.

The tail to the left of the peak in the P_{tot} distribution presents background of non exclusive events. In a fraction of events there are not reconstructed large angle tracks. These tracks manifest itself as a number of peripheral hits in the proportional chambers just after the target box. To improve the exclusivity of the sample the short track cut is additionally imposed to the events.

Due to anti-coincidence of BK1 and BK2 an event with a charged particle intersecting any of them is normally rejected at trigger level. We apply an extra requirement to the selected events that none of reconstructed tracks passes through a circular region centered at nominal position of the BK1(2) with a larger diameter of 80 mm. It is aimed to account for possible inefficiency of the counters and uncertainty in their positioning.

The Ch-28 detector is used in a threshold regime for the charged particles identification. Selected events are required to have a superiority of the $K^+K^-\pi^+\pi^-$ hypothesis over the $4\pi^\pm$ one with a ratio of their likelihoods $Lk(2K2\pi)/Lk(4\pi) > \alpha_0$. The parameter α_0 controls both PID efficiency and purity. The particular value $\alpha_0 = 2$ is chosen as a compromise between an improvement in distinction of the ϕ signal and yet acceptable events statistics.

The K^+K^- and $\pi^+\pi^-\pi^0$ invariant mass spectra (Figures 2,3) show up clean peaks centered within 1 MeV at the $M_{\phi(1020)}$ and $M_{\omega(783)}$ masses ([1]) respectively, sitting on substantial background. With a kinematic 1C fit to the π^0 mass applied to energies of two γ the ω peak is narrowed. The 2D distribution on the invariant masses $M_{3\pi}$ and M_{2K} reveals a quite clean signal of the associative production of the ω and ϕ , with less background (Figure 4).

4. General features of the $\omega\phi$ system

The signal events of the reaction (1), 1054 in total, are selected within the ellipse on the $(M_{3\pi}, M_{2K})$ plane:

$$r_{2M}^2 = (M_{3\pi} - M_\omega)^2 / (2\sigma_\omega)^2 + (M_{2K} - M_\phi)^2 / (2\sigma_\phi)^2 \leq 1 \quad (2)$$

with $\sigma_\phi = 4.4$ MeV and $\sigma_\omega = 10$ MeV.

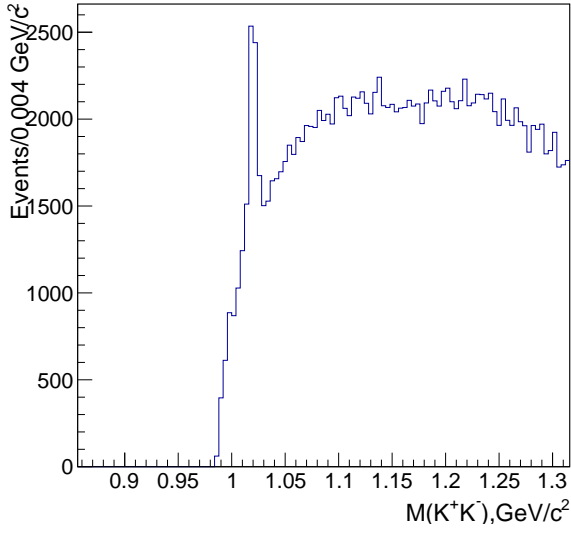


Figure 2. Invariant mass spectrum for K^+K^-

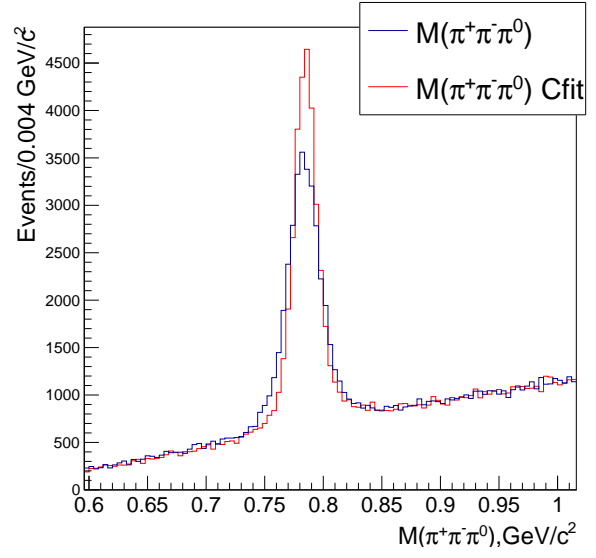


Figure 3. Invariant mass spectrum for $\pi^+\pi^-\pi^0$ with (red) and without (blue) 1C fit to the π^0 mass

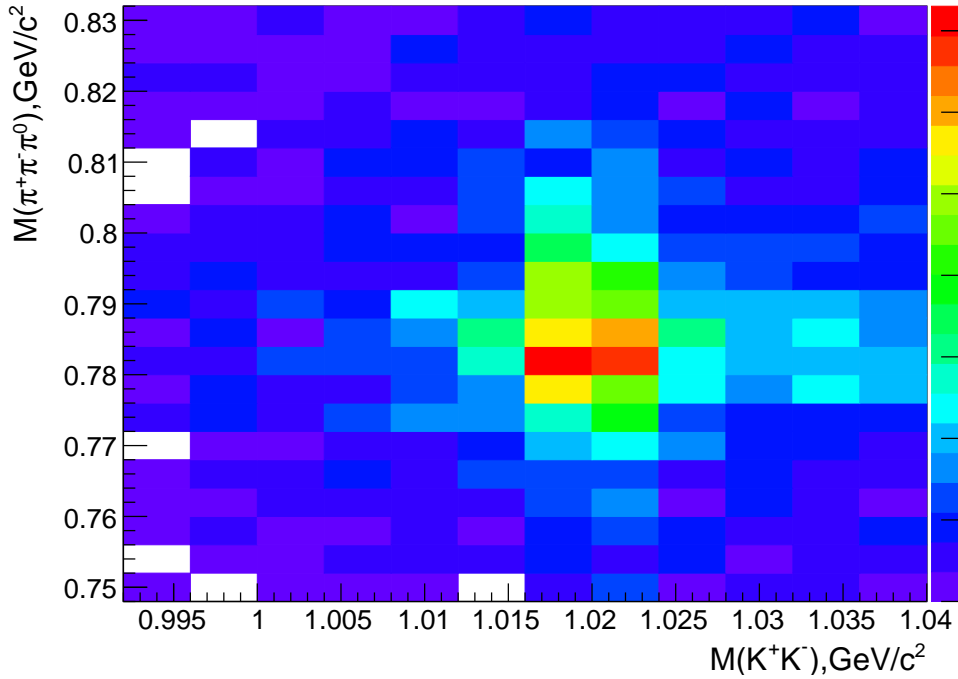


Figure 4. Invariant mass of $\pi^+\pi^-\pi^0$ vs invariant mass of K^+K^-

The linearly increasing distribution of the events on the

$$\lambda = \frac{|p_{\pi^-}^{\vec{}} \times p_{\pi^+}^{\vec{}}|^2}{\lambda_{max}}, \quad (3)$$

where $\lambda_{max} = Q^2(Q^2/108 + m_{\pi}Q/9 + m_{\pi}^2/3)$, $Q = T_{\pi^+} + T_{\pi^-} + T_{\pi^0}$, with pions momenta $p_{\pi}^{\vec{}}$ and kinetic energies T_{π} being in the 3π c.m.s., is characteristic for the $\omega \rightarrow 3\pi$ (Figure 5). Some deviations from expected shape can be attributed to non- ω background, see below.

The spectrum of the invariant mass $M_{2K3\pi}$, designated further as $M_{\omega\phi}$, is sharply peaked near the threshold. This peculiarity is of major interest of the study. On the contrary, the spectrum for events from the "background" ring $1 < r_{2M}^2 \leq 2$ doesn't show this structure (Figure 6).

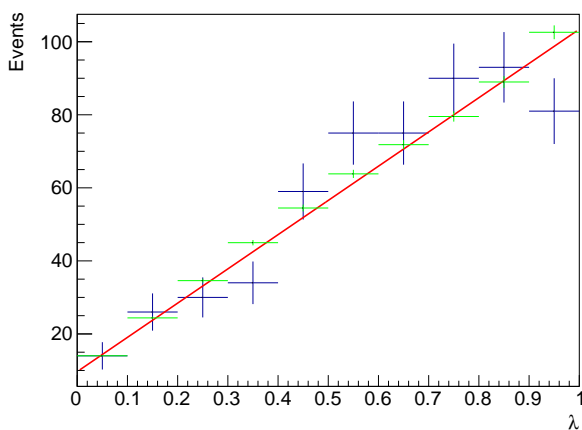


Figure 5. The events distribution on the λ (Eq. 3) for experimental data (blue) and simulated with the PWA (green); red line — linear fit to experimental data

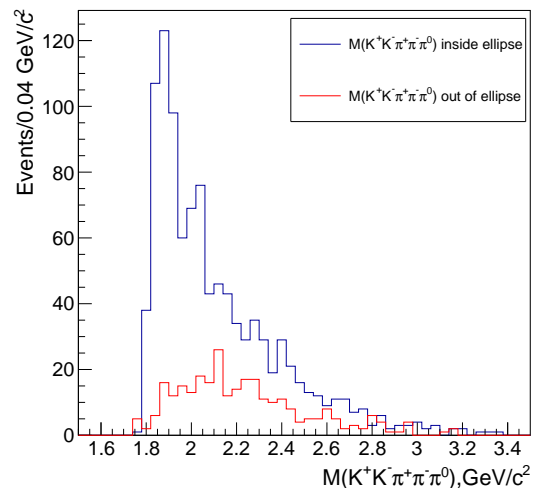


Figure 6. Invariant mass spectra of the $K^+K^-\pi^+\pi^-\pi^0$ in signal ellipse (blue) and in background ring (red)

The distribution of the events on the cosine of the angle between the normal to the ω decay plane in its c.m.s. and the kaon momentum in the ϕ c.m.s. (Figure 7) has a pronounced parabolic-like component $\propto \cos^2\theta$ expected for the decay of spinless particle to two vector particles with the $L = 0$ orbital momentum. This distribution points to a dominance of the $J^{PC} = 0^{++}$ state. To clean up a distribution on a kinematic variable which we are interested in from a not- ω background we apply bin-by-bin background subtraction, called filtering. For a given bin of the variable in question and for the M_{2K} within the ϕ band the uncut $M_{3\pi}$ distribution is fitted with a sum of polynomial background and the Gaussian signal with fixed σ_{ω} and M_{ω} . The fitted number of the signal events, N_{ω} , plotted as a function of the binned variable value, corresponds to background-free distribution.

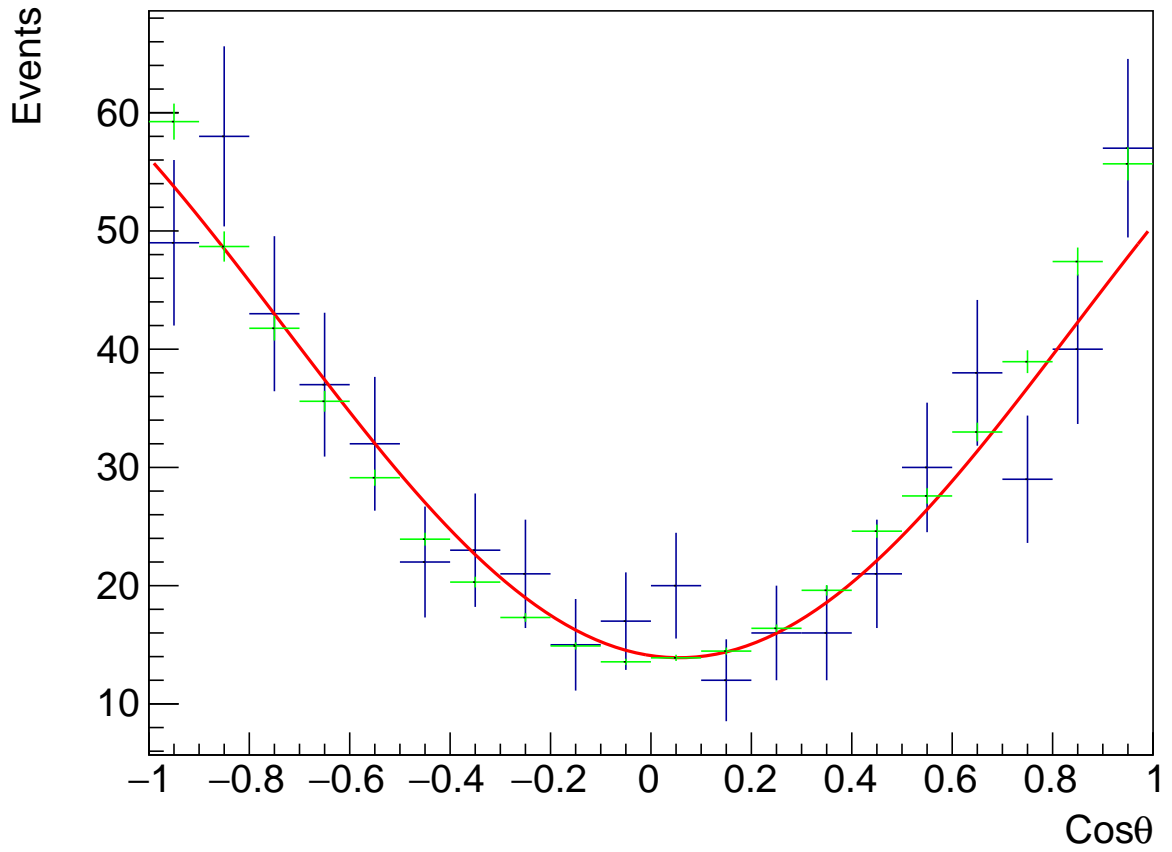


Figure 7. The events distribution on the cosine of the angle between the normal to the plane of the ω decay and the K^+ momentum in the ϕ rest frame for experimental data (blue) and simulated with the PWA result (green); red line - fit to experimental data with the function $p_1 + p_2 \cdot \cos^2 \theta$

Background subtracted t' spectrum is shown in Figure 8, where $t' = |t| - t_{min}$ ¹. Due to t_{min} smallness the difference between the t' and $-t$ can be neglected in our conditions.

The system under study, being neutral with positive G-parity, can be produced via one pion exchange. The fit to the distribution with the shape

$$\frac{dN}{dt} \propto \frac{t e^{-a_t t}}{(t - m_\pi^2)^2}$$

gives the slope $a_t = 4.3 \pm 0.5$ (stat.) GeV^{-2}

The background subtracted P_{tot} spectrum before the "exclusivity cut" is shown in the Figure 9. Also, the filtering of these spectra with respect to the non- ϕ background was

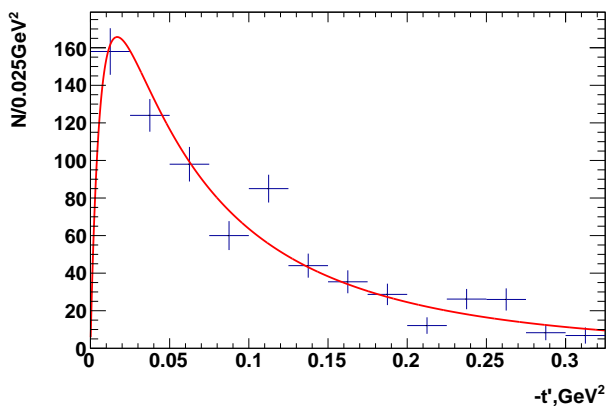


Figure 8. The t' filtered spectrum

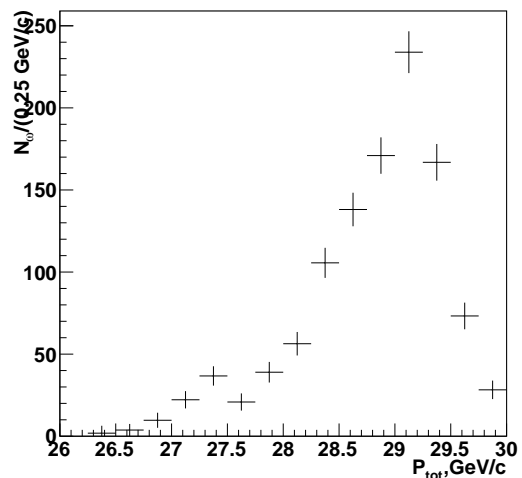


Figure 9. The P_{tot} filtered spectrum

performed, with the $M_{3\pi}$ being in the ω band. The results of two filtering are compatible.

5. Partial Wave Analysis

A mass-independent partial wave analysis of the $\omega\phi$ system was performed in 60 MeV bins in the range of invariant mass from 1.78 to 3.4 GeV. The t' is in the range from 0 to 1 GeV^2 without binning. It is essentially two-particle PWA with narrow intermediate not-interfering resonances ω and ϕ . No symmetrization w.r.t. the particles permutations is needed what distinguishes this analysis from the similar PWA of the $\omega\omega$ system in [9].

The optimization of the complex production amplitudes T_i^η was performed for each $\omega\phi$ mass bin using the extended maximum-likelihood method with the functional of the form

$$\log \mathcal{L} = \sum_k \log \sum_{\eta=\pm 1} \left| \sum_i T_i^\eta A_i^\eta(\tau_k) \right|^2 - \sum_{\eta=\pm 1} \sum_{i,j} T_i^\eta T_j^{\eta*} \int A_i^\eta(\tau) A_j^{\eta*}(\tau) \zeta(\tau) d\tau \quad (4)$$

¹ t_{min} is a designation for the $-t(M, P_{beam})|_{max}$

The index i enumerates amplitudes in two non-interfering blocks with definite "reflectivity" $\eta = \pm 1$ w.r.t. the production plane of the reaction. It is known that at high energy "reflectivity" corresponds to the "natural" and "unnatural" parity exchange (NPE and UPE) in the t -channel. This structure of the likelihood corresponds to so called "rank 1" fit.

The custom PWA program calculates first and second derivatives of $\log \mathcal{L}$ over parameters T_i^η analytically, which gives fast fit convergence and good covariance matrix.

Decay amplitudes $A_i^\eta(\tau_k)$ are calculated for each event, τ means coordinates of the phase space. The construction of the amplitudes is based on the non-relativistic spin formalism developed by Zemach in [10] and extended to the case of two particles with non-zero spins.

In our case at first two tensors of rank $j = 1$ are constructed from 3-vectors of the momentum of one of the kaons in the ϕ c.m.s (denoted as \vec{q}_1) and of the normal to ω decay plane (denoted as \vec{q}_2) respectively.

From these an S -rank tensor is constructed, symmetric and traceless for $S \geq 2$, corresponding to total intrinsic spin of two vector particles. The tensor built on momentum of one of two particles in their overall rest frame corresponds to an orbital angular momentum L between them. Finally, L and S tensors are coupled to obtain resulting tensor of rank J , which is further projected according to a projection $0 \leq M \leq J$ with respect to the beam direction in the Gottfried-Jackson system. The full notation for the wave is $J^{PC}M^\eta LS$. As an example, the amplitude $0^{++}0^-00$ has the structure $T \propto (\vec{q}_1 \cdot \vec{q}_2)$.

To account for the line shapes of the ω and ϕ the amplitudes include square roots of corresponding Gaussian functions of the $M_{3\pi}$ and M_{2K} . This helps to separate the not- ω and/or not- ϕ background.

For an effective collection of backgrounds and imperfections of the PWA model an exceptional quasi-amplitude FLAT is added. It uniformly populates five-particles phase space ($A \propto \text{const}(\tau)$). It enters in Eq. (4) as a separate block of the size 1x1.

The matrix of the so-called normalization integrals in the second term of the Eq. (4) contains an acceptance function $\zeta(\tau)$. The amplitudes are normalized as $\int |A_i^\eta|^2 d\tau = 1$. This provides acceptance-corrected wave intensities $I_i^\eta = |T_i^\eta|^2$ expressed in number of produced events, with relative phases $\phi_i^\eta - \phi_j^\eta = \arg(T_i^\eta T_j^{\eta*})$.

The integrals are calculated once before the fit procedure with the Monte-Carlo (MC) technique. The MC simulation of the setup and particles passage through it is based on the Geant4 10.5 package [11]. The reconstruction and selection procedures are applied to the simulated data as if it were real data.

The analysis is based on data taken during four runs in 2013–2015. The total number of the beam particles passed through the beam telescope over the live time of the experiment is about $2.3 \cdot 10^{11}$. The experiment performance was generally the same, with minor differences in details, such as beam momentum (within 0.5 GeV), positioning of detectors (within 1 cm) and others. Separate MC models were used for all significant time periods.

It was checked that both the general characteristics of the event samples and the results of the PWA are compatible for different runs. Then the combined PWA of the summary data was performed. For that the summary MC sample was used with the

input statistics for separate runs being proportional to the number of registered events in the run divided by the corresponding efficiency. This means an averaging of the runs efficiencies with weights proportional to the number of produced events in each run.

A small set of waves turned out to be enough to fit the data. They are: FLAT, $0^{++}0^{-}00$, $2^{++}0^{-}02$, $0^{-+}0^{+}11$. No one can be excluded from the fit without substantial deterioration of the fit quality. The scalar wave $J^{PC} = 0^{++}$ dominates among them with a peak at threshold. The tensor wave 2^{++} also exhibits some peaking behaviour but it is much less pronounced. The rest two waves are small and smooth.

To check the stability of the analysis with respect to our choice of α_0 the PWA was redone with the $\alpha_0 = 1$. and $\alpha_0 = 4$. The resulting waves stay stable within statistical errors. In the absence of an MC model for a mis-identification background we consider this as an evidence of its smallness.

To reveal a role of non- $\omega\phi$ background the PWA with a larger ellipse cut (Eq. 2) with $\sigma_\phi = 8.8$ MeV and $\sigma_\omega = 22$ MeV was performed. The only statistically significant change in wave intensities is an increase of the FLAT wave which roughly follows the increase of the circle area. From this we conclude that the background dominates in FLAT.

The major contribution to the system under study is from the unnatural parity exchange (UPE) waves which is in favour of the hypothesis of the one pion exchange (OPE) production mechanism. To suppress the contributions from alternative processes with wider t -distribution, the final analyses was performed with additional cut $t' < 0.15$ GeV² leaving 596 input events. The resulting PWA demonstrates a suppression of the FLAT and the $J^{PC} = 0^{-+}$ waves, further increasing the dominance of the scalar signal.

6. Results and discussion

The intensities of the waves in the final PWA results are presented in Fig. 10. The overall acceptance of the setup varies slowly with the $\omega\phi$ mass between 5.1% and 6.7%. A comparison of some distributions for the Monte-Carlo events simulated according to the PWA with the real data are seen in Fig. 5, 7.

Below we compare the characteristics of the reactions $\pi^- Be \rightarrow A'\omega\phi$ and $\pi^- Be \rightarrow A'\omega\omega$. Results of the analysis of the $\omega\omega$ system on VES setup at 28 GeV nominal momentum are used [9, 4]. Values for $\omega\omega$ system are marked as "28", values for $\omega\phi$ one as "29".

A dominant state in a wide mass range of the $\omega\omega$ is $J^P = 2^+$. The intensity of the 0^+ is significant and without prominent structures.

We extract the intensity of the $0^{++}0^{-}00$ from the Figure 4 of [4] and the total intensity taken as a sum of UPE and NPE waves from the Figure 4 of [9]. From these the relative contribution of the scalar wave $N_{\omega\omega,28}^{0^+}/N_{\omega\omega,28}$ is derived as a function of the mass.

To relate two experiments the observed mass spectrum in the current one $N_{\omega\omega,29}^{obs}$ (Figure 11) needs to be corrected by the efficiency $\epsilon_{29}(M_{\omega\omega})$. It is estimated from a Monte Carlo simulation. The kinematics is generated using the experimental t -distribution and the known distribution on the λ for two ω decays. As for the angular distributions, they are simulated according to two states, the $J = 0$ which we are interested in, and

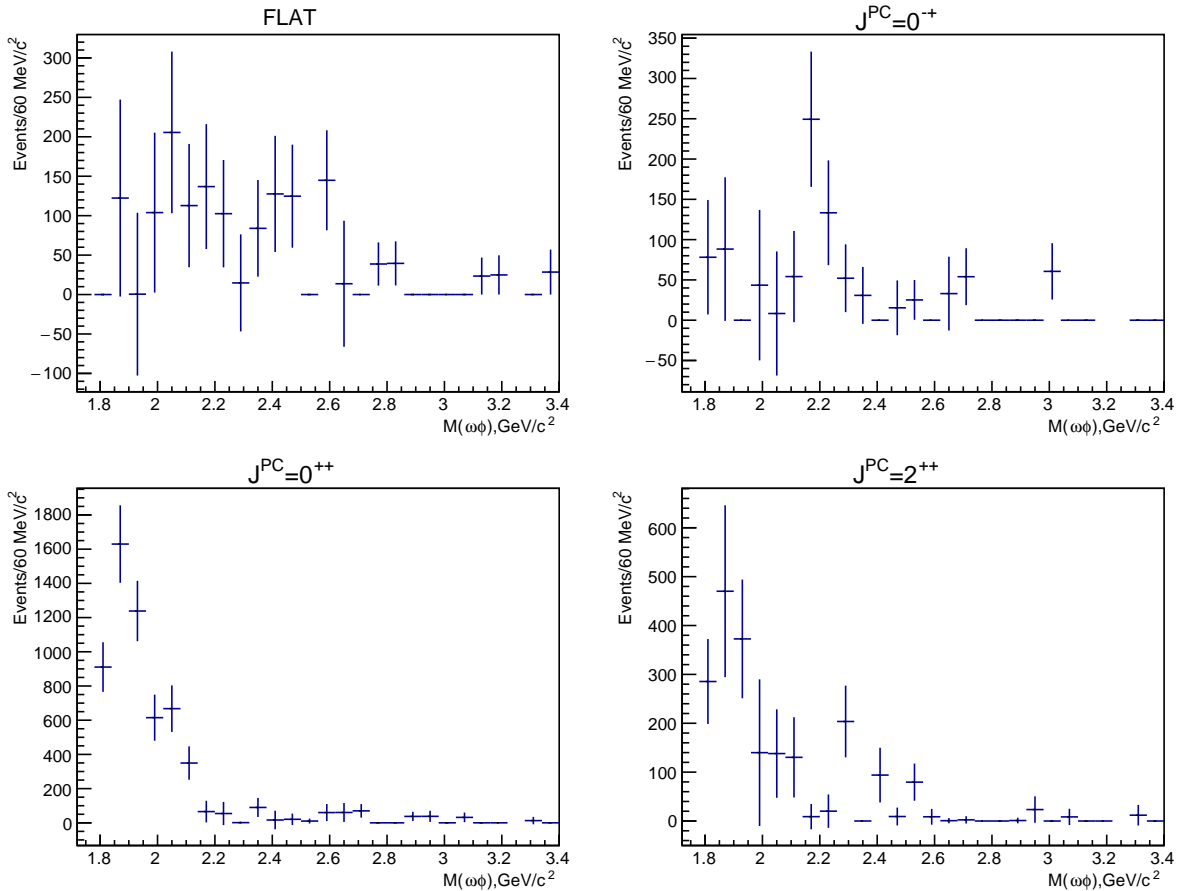


Figure 10. Intensities of the most significant waves in the PWA fit

alternatively the dominating $J = 2$, with the orbital momentum $L = 0$ in both cases. The $\epsilon_{29} \approx 0.06$ is a weak function of the mass in the given range, its relative difference in the two simulated cases is typically less than 5%.

So the scalar wave intensity for the current experiment is

$$N_{\omega\omega,29}^{0^+}(M_{\omega\omega}) = \frac{N_{\omega\omega,29}^{obs}}{\epsilon_{29}} \cdot \frac{N_{\omega\omega,28}^{0^+}}{N_{\omega\omega,28}} \quad (5)$$

To account for a wider range $|t| < 0.20 \text{ GeV}^2$ in case of the $\omega\omega$ an additional correction factor 1.13 ± 0.03 is applied.

Finally, we get the ratio of $0^{++}0^{-00}$ wave intensities in the $\omega\phi$ and $\omega\omega$ systems in the range $|t| < 0.15 \text{ GeV}^2$:

$$R = \frac{N_{\omega\phi,29}^{0^+}}{N_{\omega\omega,29}^{0^+}} \cdot \frac{Br(\omega \rightarrow \pi^+\pi^-\pi^0)}{Br(\phi \rightarrow K^+K^-)} \quad (6)$$

It is presented as function of mass in Figure 12 in blue. The errors comprise uncertainties of all factors in the (5), (6), the largest are in the waves intensities.

Also, the ratio R_A of these intensities divided each by the corresponding decay momentum q_ω in the c.m.s. of the $M_{\omega\omega(\phi)} \rightarrow \omega\omega(\phi)$ is calculated to exclude the decay phase space factor. The first bin is omitted due to very sharp momentum dependence near threshold. The averaging over the mass range 1.84 – 2.08 GeV gives the value $\langle R_A \rangle = 3.24 \pm 1.0$.

Much lower ratio R for the $2^{++}0^{-02}$ which was obtained similarly to (5), (6) is shown for comparison in Figure 12 in red.

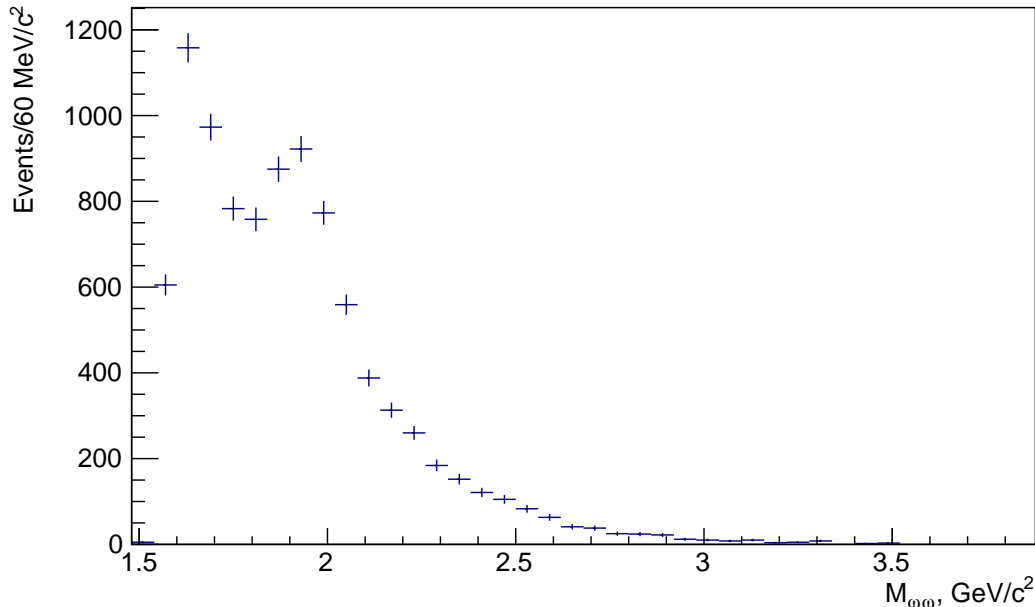


Figure 11. The invariant mass spectrum of the $\omega\omega$ system in the current experiment

The structure in the scalar wave resembles that in the radiative J/ψ decay to the $\omega\phi$ in [2, 3]. Those results are listed in the [1] in the entry for the $f_0(1710)$, where one gets $R_{Rad.Dec.} = \frac{Br(J/\psi \rightarrow \gamma f_0(1710) \rightarrow \gamma \omega \phi)}{Br(J/\psi \rightarrow \gamma f_0(1710) \rightarrow \gamma \omega \omega)} = 0.8 \pm 0.4$.

To compare our result with this we calculate the ratio in the current experiment over the whole mass range between 1.6 and 2.1 GeV: $R_{ChEx} = 0.7 \pm 0.15$. The values are in a good agreement with each other.

6.1. Discussion

Both the shape of the scalar intensity in the $\omega\phi$ channel and its ratio to that in the $\omega\omega$ one are consistent in the radiative J/ψ decays and in the charge exchange reaction. We assume that one and the same object is observed in both cases, namely the $f_0(1710)$.

As the signal in the $\omega\phi$ is on the tail of the $f_0(1710)$ the determination of the resonance mass M_R and width Γ_R is very model dependent in this channel and so unreliable. In the Figure 13 we show an example of a fit to the wave intensity with the function

$$\frac{dN}{dM} = C \cdot ((M_R^2 - M^2)^2 + M_R^2 \Gamma_R^2)^{-2} \cdot \frac{2q_\omega(M)}{M} \quad (M > M_\omega + M_\phi) \quad (7)$$

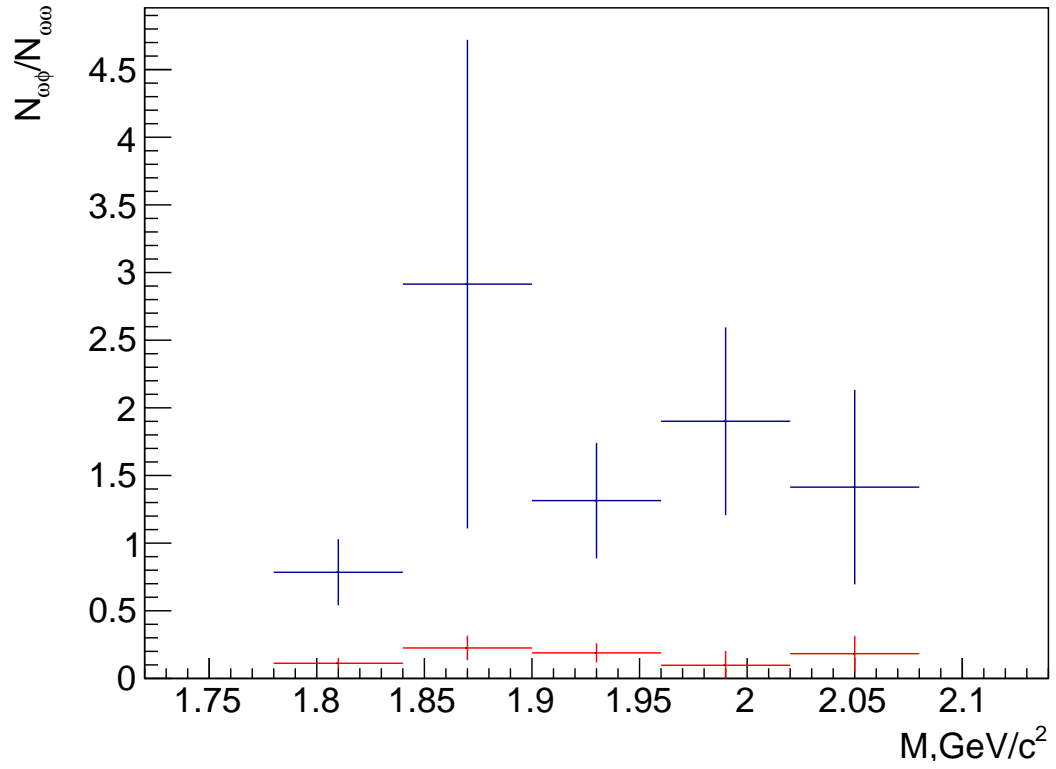


Figure 12. The ratio of waves intensities in $\omega\phi$ and $\omega\omega$ systems: $J^P = 2^+$ (red) and $J^P = 0^+$ (blue). Branching fractions of $\omega \rightarrow \pi^+\pi^-\pi^0$, $\phi \rightarrow K^+K^-$ are taken into account

The width was taken in the form: $\Gamma_R = \Gamma_0 + \Gamma_{\omega\phi} \cdot 2q_\omega/M$. The Γ_0 accounts for decay channels which are far from the threshold and the $\Gamma_{\omega\phi}$ is for the near-threshold channel. The results of the fit are $M_R = (1.780 \pm 0.050)$ GeV and $\Gamma_0 = (0.150 \pm 0.020)$ GeV. Uncertainty comes from model variation and fit range. Next we use as $f_0(1710)$ parameters $M = 1733_{-7}^{+8}$ MeV and $\Gamma = 150_{-10}^{+12}$ MeV from [1].

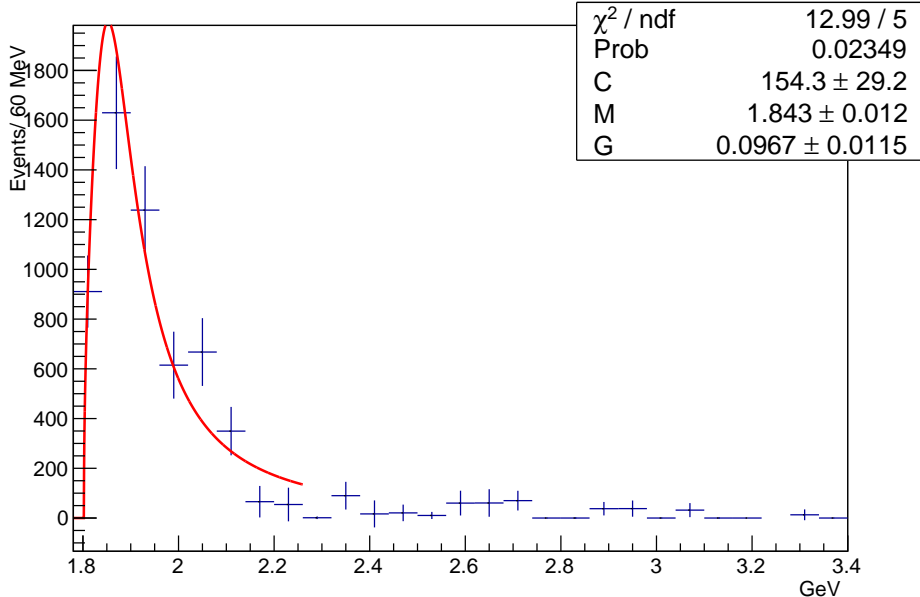


Figure 13. The 0^+ intensity fitted with a model function, see text

With a given number of events in the scalar wave below 2.1 GeV which constitutes about 0.52 of the total number of events and taking into account the branching fractions for the ω and ϕ decays ([1]) we get the cross-section

$$\sigma(\pi^- Be \rightarrow A f_0(1710)) \cdot Br(f_0(1710) \rightarrow \omega\phi) = 98 \pm 4(\text{stat.}) \pm 7(\text{syst.}) \text{ nb} \quad (8)$$

The systematic error is taken as the quadratic sum of contributions from uncertainties in the efficiency, cross section normalization and two branching fractions.

For the further analysis we need a cross-section on the proton. A number of theoretical and experimental works relates cross-sections of charge-exchange reactions on the proton and nuclei ([12, 13, 14]). The dependence in the form $\sigma \propto Z_{eff}$ can be used. From the experimental data [14] for isoscalar productions in charge exchange reactions at the beam momentum 39 GeV/c we evaluate $Z_{eff} = Z^{0.73 \pm 0.03}$, so we take the $Z_{eff} = 2.7 \pm 0.2$ which results in the $\sigma(\pi^- p \rightarrow n f_0(1710)) \cdot Br(f_0(1710) \rightarrow \omega\phi) = 39 \pm 4.4$ nb. The systematic uncertainty dominates in the combined error.

Next we proceed to the calculation of the product of $Br(f_0 \rightarrow \pi\pi)$ and $Br(f_0 \rightarrow \omega\phi)$ using the OPE approximation for the production of a resonance X , decaying to a given channel ([15, 16]):

$$\sigma(\pi^- p \rightarrow nX) \cdot Br(X \rightarrow \text{channel}) =$$

$$40.4 \text{ mb} \cdot (2J + 1) \cdot \frac{2}{3} Br(X \rightarrow \pi\pi) \cdot Br(X \rightarrow \text{channel}) \cdot M_X \cdot \Gamma / P_{beam}^2 \cdot C(\beta)$$

where $C(\beta) = \int \frac{t \cdot e^{\beta(t-m_\pi^2)}}{(t-m_\pi^2)^2} dt$ and $2/3$ is isotopic factor. This approximation is widely used for analysis of charge-exchange reactions with the UPE dominance. Its systematical uncertainty is estimated as 20% ([17])

In our case $J = 0$, $\beta = 4.3 \text{ GeV}^{-2}$, the upper integration limit is $|t|_{max} = 0.15 \text{ GeV}^2$

Using $M_X \cdot \Gamma = 0.260 \pm 0.021 \text{ GeV}^2$ this leads to $Br(f_0 \rightarrow \pi\pi) \cdot Br(f_0 \rightarrow \omega\phi) = (4.8 \pm 1.2) \cdot 10^{-3}$. Accounting for the $Br(J/\psi \rightarrow \gamma f_0(\pi\pi)) \cdot Br(J/\psi \rightarrow \gamma f_0(\omega\phi)) = (9.5 \pm 2.6) \cdot 10^{-8}$ from [1] we get the $Br(J/\psi \rightarrow \gamma f_0(1710)) = (4.46 \pm 0.82) \cdot 10^{-3}$. When compared with the experimental value $Br(J/\psi \rightarrow \gamma f_0) \cdot Br(f_0(1710) \rightarrow 5 \text{ channels}) = (2.13 \pm 0.18) \cdot 10^{-3}$ this leaves for the unregistered channels $Br(f_0 \rightarrow 4\pi, \eta\eta', \pi\pi KK \dots) = (2.23 \pm 0.84) \cdot 10^{-3}$.

Comparison of obtained value for the $Br(J/\psi \rightarrow \gamma f_0(1710))$ with the value $(3.8 \pm 0.9) \cdot 10^{-3}$ calculated in [18] within the lattice model for a scalar glueball indicates the presence of a significant or even dominating glueball component in the $f_0(1710)$.

To illustrate the properties of the scalar in question we refer also to a model [19] where the branching of a heavy vector quarkonium radiative decay to a resonance R with spin J is proportional to the width of the R decay to two gluons:

$$Br(Q\bar{Q}_V \rightarrow \gamma R_J) / Br(Q\bar{Q}_V \rightarrow \gamma gg) = K_J(m_R/M_V) m_R \Gamma_R Br(R_J \rightarrow gg) / M_V^2$$

where $K_J(m_R/M_V)$ is a function of J and m_R/M_V . Using $K_0(m_{f_0(1710)}/M_{J/\psi}) = 1.16$ from [19], $Br(J/\psi \rightarrow \gamma gg) = 0.088 \pm 0.011$ ([1]) and $Br(J/\psi \rightarrow \gamma f_0(1710))$ obtained here one gets $Br(f_0(1710) \rightarrow gg) = 1.66 \pm 0.39$. The error shown is mainly due to the uncertainties of J/ψ radiative decays branchings and the OPE model and doesn't include a systematics of the model [19].

In [20] there are convincing evidences in favour of splitting of the $f_0(1710)$ to two resonances, of which only the heavier one contributes to the $\omega\phi$ channel. The values for this $f_0(1770)$ are given: $M = 1765 \pm 15 \text{ MeV}$, $\Gamma = 180 \pm 20 \text{ MeV}$, $Br(J/\psi \rightarrow \gamma f_0(1770) \rightarrow \pi\pi) = (2.4 \pm 0.8) \cdot 10^{-3}$, $Br(J/\psi \rightarrow \gamma f_0(1770) \rightarrow \omega\phi) = (2.2 \pm 0.4) \cdot 10^{-3}$. Then one finds $Br(f_0 \rightarrow \pi\pi) \cdot Br(f_0 \rightarrow \omega\phi) = (3.9 \pm 1.0) \cdot 10^{-3}$, $Br(J/\psi \rightarrow \gamma f_0) = (3.68 \pm 0.84) \cdot 10^{-3}$, $Br(f_0 \rightarrow 4\pi, \eta\eta', \pi\pi KK \dots) = (1.55 \pm 0.86) \cdot 10^{-3}$, and $Br(f_0 \rightarrow gg) = 1.12 \pm 0.32$. These values don't change the conclusion on a large glueball component in the considered meson.

7. Conclusion

The reaction $\pi^- Be \rightarrow A \omega\phi$ was studied at the beam momentum 29 GeV. The $J^{PC} = 0^{++}$ state dominates in the $\omega\phi$ system. When compared with the $\omega\omega$ case, the signal is characterized with a large violation of the OZI rule. Namely, the average ratio of the intensities of the scalar waves in two systems with the phase space factors taken out is $\langle R_A \rangle = 2.9 \pm 1.0$. The signal in the $\omega\omega$ and $\omega\phi$ channels can be attributed to the known $f_0(1710)$. The cross-section

$$\sigma(\pi^- Be \rightarrow A f_0(1710)) \cdot Br(f_0(1710) \rightarrow \omega\phi) = 98 \pm 4(stat.) \pm 7(syst.) \text{ nb} \quad (9)$$

is measured for $|t'| < 0.15 \text{ GeV}^2$. Using the OPE model for the reaction $\pi^- p \rightarrow n f_0(1710)$ and relative fractions for the radiative J/ψ decays the branching fraction is found to be: $Br(J/\psi \rightarrow \gamma f_0(1710)) = (4.4 \pm 0.8) \cdot 10^{-3} ((3.7 \pm 0.8) \cdot 10^{-3})$ with the table (alternative) parameters for the $f_0(1710)$ ($f_0(1770)$). The large value for the $Br(J/\psi \rightarrow \gamma f_0(1710/1770))$ is an evidence of a large glueball component in the $f_0(1710/1770)$ state.

This work was done with the use of the IHEP (Protvino) Central Linux Cluster. The work is partially supported with the RFBR grant 20-02-00246. Authors are grateful to A. Solodkov for reading and correcting the manuscript.

References

- [1] Workman, R. L., *et al.*: Review of Particle Physics. PTEP **2022**, 083-01 (2022)
- [2] Ablikim, M., *et al.*: Observation of a near-threshold enhancement in the omega phi mass spectrum from the doubly OZI suppressed decay $J/\psi \rightarrow \gamma \omega \phi$. Phys. Rev. Lett. **96**, 162002 (2006)
- [3] Ablikim, M., *et al.*: Study of the near-threshold $\omega\phi$ mass enhancement in doubly OZI-suppressed $J/\psi \rightarrow \gamma\omega\phi$ decays. Phys. Rev. D **87**(3), 032008 (2013)
- [4] Ivashin, A., *et al.*: Evidence for a scalar meson resonance in the $\pi^- p \rightarrow n \omega$ phi reaction. AIP Conf. Proc. **1257** (1), 262–266 (2010)
- [5] Kholodenko, M.S.: Particle identification with the Cherenkov detector in the VES experiment. JINST **15**(07), 07024 (2020).
- [6] Dorofeev, V.A., Ivashin, A.V., Kalendarev, V.V., Katchaev, I.A., Konstantinov, V.F., Matveev, V.D., Polyakov, B.F., Sugonyaev, V.P., Kholodenko, M.S., Khokhlov, Y.A.: A new electromagnetic calorimeter for the updated VES setup. Instrum. Exp. Tech. **59**(5), 658–665 (2016)
- [7] Ivashin, A.V., Khokhlov, Y.A., Matveev, V.D.: Upgraded data acquisition system for the VES setup. Technical aspects. Preprint in Russian at <http://web.ihep.su/library/pubs/2010/ps/2010-10.pdf> (2010)
- [8] Ekimov, A., Fedorchenko, V., *et al.*: The VES detector control system. Preprint in Russian at <http://web.ihep.su/library/pubs/2013/ps/2013-2.pdf> (2013)
- [9] Amelin, D.V., *et al.*: Resonances in the omega omega system. Phys. Atom. Nucl. **69**, 690–698 (2006)
- [10] Zemach, C.: Three pion decays of unstable particles. Phys. Rev. **133**, 1201 (1964)
- [11] Agostinelli, S., *et al.*: GEANT4—a simulation toolkit. Nucl. Instrum. Meth. A **506**, 250–303 (2003)
- [12] Kolbig, K.S., Margolis, B.: Particle production in nuclei and unstable particle cross-sections. Nucl. Phys. B **6**, 85–101 (1968)
- [13] Guisan, O., Bonamy, P., Le Du, P., Paul, L.: Study of $\pi^- p \rightarrow \pi^0 n$ and $\pi^- p \rightarrow \eta n$ reactions in nuclei at 7.82 gev/c. Nucl. Phys. B **32**, 681–690 (1971)
- [14] Apokin, V.D., *et al.*: DETERMINATION OF THE CROSS-SECTION OF THE PROCESS $\pi^+ \pi^- \rightarrow \pi^0 \pi^0$ IN THE DIPION MASS RANGE $0.55\text{-GeV} < M < 2\text{-GeV}$ FROM THE REACTION $\pi^- p \rightarrow \pi^0 \pi^0 n$ AT 39.1-GeV/c. Sov. J. Nucl. Phys. **49**, 278 (1989)

- [15] Chew, G.F., Low, F.E.: Unstable particles as targets in scattering experiments. Phys. Rev. **113**, 1640–1648 (1959)
- [16] Williams, P.K.: Extrapolation model for pi pi scattering. Phys. Rev. D **1**, 1312–1318 (1970).
- [17] Hyams, B., *et al.*: t Dependence and Production Mechanisms of the rho, f and g Resonances from pi- p -> pi- pi+ n at 17.2-GeV Phys. Lett. B **51**, 272–278 (1974)
- [18] Gui, L.-C., Chen, Y., Li, G., Liu, C., Liu, Y.-B., Ma, J.-P., Yang, Y.- B., Zhang, J.-B.: Scalar Glueball in Radiative J/ψ Decay on the Lattice. Phys. Rev. Lett. **110**(2), 021601 (2013)
- [19] Close, F.E., Farrar, G.R., Li, Z.-p.: Determining the gluonic content of isoscalar mesons. Phys. Rev. D **55**, 5749–5766 (1997)
- [20] Sarantsev, A.V., Denisenko, I., Thoma, U., Klempt, E.: Scalar isoscalar mesons and the scalar glueball from radiative J/ψ decays. Phys. Lett. B **816**, 136227 (2021)

Рукопись поступила 4 апреля 2023 г.

Препринт отпечатан с оригинала-макета, подготовленного авторами.

В.А. Дорофеев и др.

Наблюдение $f_0(1710)$ мезона в системе $\omega\phi$ в пион- Be взаимодействии при импульсе 29 ГэВ.

Оригинал-макет подготовлен с помощью системы **L^AT_EX**.

Подписано к печати 05.04.2023 Формат 60 × 84/16. Цифровая печать.
Печ.л. 1,4. Уч.-изд.л. 1,9. Тираж 60. Заказ 7. Индекс 3649.

НИЦ «Курчатовский институт» – ИФВЭ
142281, Московская область, г. Протвино, пл. Науки, 1

www.ihep.ru; библиотека <http://web.ihep.su/library/pubs/all-w.htm>

Индекс 3649

П Р Е П Р И Н Т 2023–6,
НИЦ «Курчатовский институт» – ИФВЭ, 2023
